PCCP

Cite this: *Phys. Chem. Chem. Phys.*, 2011, **13**, 16987–16998

www.rsc.org/pccp

PERSPECTIVE

Excited-state calculations with TD-DFT: from benchmarks to simulations in complex environments

Denis Jacquemin,*[a] Benedetta Mennucci*[b] and Carlo Adamo*[c]

Received 30th June 2011, Accepted 5th August 2011
DOI: 10.1039/c1cp22144b

In this perspective, we present an overview of recent progress on Time-Dependent Density Functional Theory (TD-DFT) with a specific focus on its accuracy and on models able to take into account environmental effects, including complex media. To this end, we first summarise recent benchmarks and define an average TD-DFT accuracy in reproducing excitation energies when a conventional approach is used. Next, coupling of TD-DFT with models able to account for different kinds of interactions between a central chromophore and nearby chemical objects (solvent, organic cage, metal as well as semi-conducting surface) is investigated. Examples of application to excitation properties are presented, allowing to briefly describe several recent computational strategies. In addition, an extension of TD-DFT to describe a phenomenon involving interacting chromophores, *e.g.* the electronic energy transfer (EET), is presented to illustrate that this methodology can be applied to processes beyond the vertical excitation. This perspective therefore aims to provide to non-specialists a flavour of recent trends in the field of simulations of excited states in "realistic" situations.

1 Introduction

The importance of processes related to electronically excited states in chemistry, physics and technology will continue to rapidly increase during the next decades. These phenomena originate from the interactions between matter and external electromagnetic fields, typically incoming light. In practice, excited-states are not only related to well-known (though far from perfectly mastered) applications (*e.g.* dyeing and chemical colours, fluorescence and phosphorescence) but also play a predominant role in energy conversion (*e.g.* solar cells, photosynthesis), biological processes (green fluorescent protein, GFP, photodynamic therapy) and are also a key to build controllable devices at the molecular scale (*e.g.* logic gates based on single-molecule photochromism). Contrary to their ground state counterparts, excited-states are short-lived, highly reactive and often coupled together, making the quest to master their manipulation a capital but extremely involved demand. In fact, even accurate and extensive descriptions of the ground-state properties, obtained through experimental or theoretical means, fell short to understand the behaviours of electronically excited compounds. Consequently, projections of the intuitive chemical notions to excited-states are bound to founder. In that framework, accurate theoretical models delivering an atomic-scale characterisation of the elemental electron processes are actively searched for, not only to complement the generally expensive and lengthy experimental measurements, but also to define strategies useful for the design of novel compounds with tailored properties.

Time-Dependent Density Functional Theory (TD-DFT), proposed 25 years ago by Runge and Gross,[1–4] is probably the most widely used theoretical approach to compute not only the transition energies but also the excited-state properties such as dipole moments and emitting geometries. This popularity, that can be illustrated by a web of science search on the topic that yields a number of contributions steadily increasing with time,[5] may be explained as the competing approaches are either less accurate or highly-demanding. On the one hand, one finds semi-empirical schemes like the purpose-made ZINDO/S approach[6] or the more general PM5 or PM6 models[7] that are lighting-fast to simulate the UV/Visible spectra but provide strongly system-dependent results.[8–12] On the other hand, there are highly-correlated *ab initio* approaches that are much more accurate than TD-DFT but suffer from a quite extreme computation cost. Amongst these schemes, CAS-PT2 and EOM-CC, the two "lighter" theories, can be applied to compounds containing *ca.* 50 atoms,[13–22] but their current implementation generally forbids a systematic inclusion of medium effects, despite the efforts achieved during

[a] *Chimie et Interdisciplinarité, Synthèse, Analyse, Modélisation (CEISAM), UMR CNRS no. 6230, BP 92208, Université de Nantes, 2, Rue de la Houssinière, 44322 Nantes Cedex 3, France. E-mail: denis.jacquemin@univ-nantes.fr*
[b] *Department of Chemistry, University of Pisa, Via Risorgimento 35, 56126 Pisa, Italy. E-mail: bene@dcci.unipi.it*
[c] *Ecole Nationale Supérieure de Chimie de Paris, Laboratoire LECIME, UMR CNRS-ENSCP no. 7575, 11, rue Pierre et Marie Curie, F-75321 Paris Cedex 05, France. E-mail: carlo-adamo@chimie-paristech.fr*

the recent years.[23–26] As it is well-recognised that excited-state properties tend to be more environmental-sensitive than their ground-state counterparts, this is a significant drawback. On the contrary extension of (TD-)DFT to incorporate bulk solvent effects date from 10 years ago,[27–31] is widely implemented in quantum packages and is routinely applied during the calculation of absorption spectra. Nevertheless, theoreticians still strive for simulating cases that require going beyond continuum approaches.[32]

Despite its successes and versatility, TD-DFT suffers from, at least, a major limitation: the reliability of the results depends significantly on the selected exchange-correlation (xc) functional. Though chemical accuracy (0.10 eV) may not yet have been reached on a systematic basis, some difficulties have been circumvented since the developments of range-separated hybrids (RSH).[33–37] These functionals incorporate a growing fraction of exact exchange with increasing inter-electronic distance, and allow us adequately model charge-transfer phenomena as well as to avoid the presence of spurious states.

In this contribution, we do not aim at providing a complete review of all existing developments and applications of (TD-)DFT, but rather to give a flavour of todays possibilities and typical accuracies using specific examples, especially those accounting for rather complex environmental situations. The interested reader might find a series of reviews on the fundamental aspects of TD-DFT and related applications in previous papers,[4,38–46] as well as in dedicated journal issues.[47,48] Following Section 2 that collates results of recent benchmarks, we focus on solvent effects for absorption and emission processes (Section 3) and deal with the impact on the same processes of interactions between the dye and a cage, a metal nanoparticles, and a surface (Sections 4.1, 4.2 and 4.3, respectively). Finally, Section 5 describes strategies to account for electronic energy transfer (EET), a problematic beyond the vertical processes as it involves interactions among excitations.

2 Benchmarks

Before describing recent developments and approaches aiming to apply TD-DFT calculations in complex media, we discuss in this section the results obtained by recent benchmarks, so to provide a picture of the expected TD-DFT accuracy in the gas-phase or in "simple" (*e.g.* aprotic solvent) environments, when a conventional linear-response (LR) approach is applied. In LR methods, the transition energies are defined as *singularities* of the frequency dependent response functions of the reference (ground) electronic state avoiding explicit calculation of the excited state wavefunction. Published assessments generally aim either to pinpoint an adequate method in the large palette of existing xc functionals or to test the relative performances of a specific (family of) xc form(s).[49–63] Besides, these works differ by three key aspects: (1) the chosen set of molecules, (2) the selected reference values and (3) the applied methodology. This diversity probably explains why a broadly accepted "best" functional remains to be identified. Consequently, we mainly focus on describing the conclusions that are relatively uniform in all investigations. Nevertheless, one should be aware that the accuracy is significantly dependent on the selected family of chromogens.

Amongst all benchmark sets, the molecular ensemble proposed by Thiel and collaborators in 2008[60,64,65] is certainly one of the most popular. Indeed, accurate vertical wave function reference values have been obtained at both the CAS-PT2 and CC3 levels for a large number of singlet and triplet excited-states, allowing comparisons on a perfectly equal footing (vertical approximation with the same geometries and basis sets).[53–55,57,59–61,63] However, as only relatively small molecules (naphthalene, isolated DNA bases...) are included in this set, some chemically-important phenomena, *e.g.* charge-transfer transitions between distant electro-active groups, remain beyond the scope of Thiel's database. In Fig. 1, we present the mean signed and absolute errors (MSE and MAE, respectively) calculated with more than 35 functionals for 103 singlet excited-states selecting Thiel's *theoretical best estimates* (TBE) as

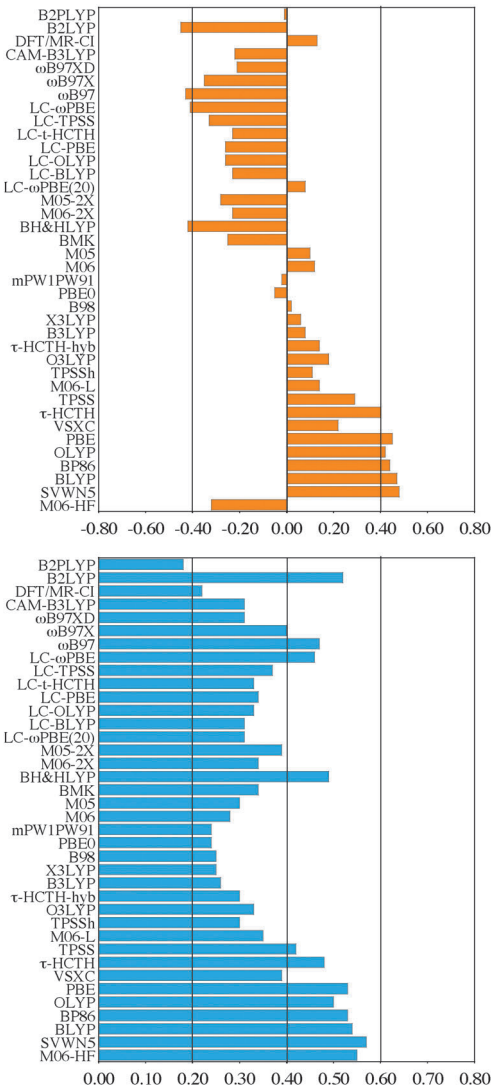

Fig. 1 MSE (top) and MAE (bottom) obtained for singlet excited-states. All values are in eV and use Thiel's theoretical best estimates (TBE) as benchmarks. Original data from ref. 53–55, 57, 59, and 61. Note that the MSE and MAE calculated for double hybrids in ref. 54 have been recomputed using the TBE as the reference.

reference values. These functionals are: M06-HF,[66] SVWN5,[67,68] BLYP,[69,70] BP86,[69,71] OLYP,[70,72] PBE,[73] VSXC,[74] τ-HCTH,[75] TPSS,[76] M06-L,[77] TPSSh,[78] O3LYP,[79] τ-HTCHh,[75] B3LYP,[80,81] X3LYP,[82] B98,[83] mPW1PW91,[84] PBE0,[85,86] M06,[87] M05,[88] BMK,[89] BHHLYP,[90] M06-2X,[87] M05-2X,[91] LC-ωPBE(20),[55] LC-BLYP,[34,69,70] LC-OLYP,[34,70,72] LC-PBE,[34,73] LC-τ-HTCHh,[34,75] LC-TPSS,[34,76] LC-ωPBE,[36,92] ωB97,[93] ωB97X,[93] ωB97XD,[94] CAM-B3LYP,[95] DFT/MR-CI,[53,96,97] B2LYP[98,99] and B2PLYP.[98,99] Though all data have been consistently obtained with the diffuse-less TZVP basis set, recent investigations hint that the selection of a much larger basis set, such as *aug*-cc-pVTZ, would have a limited impact on the presented statistical values.[57,60] For the singlets, one notes a clear evolution along the exact exchange ratio: pure density functionals undershoot transition energies, whereas global hybrids including a large (> 50%) share of exact exchange as well as range-separated hybrids relying on an attenuation parameter exceeding 0.3 a.u. suffer from the opposite error. Overall, the smallest deviations (*ca.* 0.20 eV) are reached with the two most refined schemes, namely, Grimme's B2PLYP,[99] a double-hybrid that includes a specific CIS(D)-like[100] corrections for the excited-state part,[54] and the DFT multi-reference approach proposed by Silva-Junior *et al.*[53] Global hybrids including 20–30% of exact exchange (*e.g.* B3LYP,[80,81] B98,[83] PBE0[85,86] or M06)[87] yield slightly larger deviations (*ca.* 0.25 eV). Another strategy to improve the description of this set of molecules is to rely on dressed TD-DFT that allows an improved description of states presenting a significant double-excitation character, as originally shown by Burke and coworkers for butadiene and hexatriene,[101] confirmed for longer polyenes by Mazur and Wlodarczyk,[102] and recently extended to a larger set of molecules by Rubio's and Casida's groups.[63] For the 63 triplets (Fig. 2), the transition energies are almost systematically underrated by TD-DFT, the average errors tending to be larger than for singlets. In addition, no clear-cut dependence between the MSE and the DFT/HF mixing parameter(s) could be found. M06-2X,[87] BMK[89] and the DFT/MR-CI schemes have the edge for triplets with MAE smaller than 0.30 eV. It should be noted that the results collated in Fig. 1 and 2 are based on standard LR TD-DFT. More specific or purpose-oriented models, such as spin-flipping for triplets,[103] or the above-mentioned dressed TD-DFT,[63] or localized HF Kohn-Sham approach[104] might yield different results, especially for triplets.

When comparing experimental and theoretical results, the major dilemma may be expressed as: should one select very accurate values obtained on small gas-phase molecules (therefore allowing the use of large basis sets and fully adiabatic calculations, but at the price of a limited set of data) or use condensed-phase results obtained on large systems (implying additional theoretical approximations but opening the way towards more chemically-interesting systems)? Several strategies have been designed,[50–52,55,56,58] and, at least, one generic conclusion has emerged: pure density functionals tend to behave quite poorly. Indeed they generally yield much too small transition energies, *e.g.* Dierksen and Grimme reported that the BP86[69,71] GGA systematically undershoots the experimental 0–0 energy, with an average amplitude of 0.57 eV, in their set of 40 medium and large (aromatic) molecules,[50] whereas we obtained a MAE of 0.38 eV for the same functional

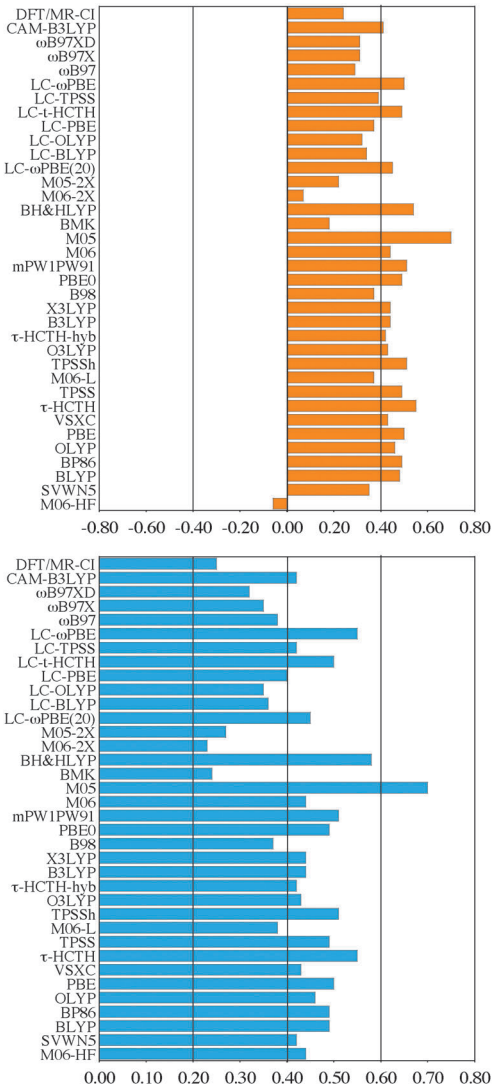

Fig. 2 MSE (top) and MAE (bottom) obtained for triplet excited-states. See caption of Fig. 1 for more details.

considering low-lying states of 500 chromogens, within a vertical scheme.[55] The errors become even more dramatic for Rydberg and charge-transfer states, an outcome well illustrated by the investigation of Tozer's group: the PBE's[73] MSE reach 0.31 eV, 1.84 eV and 2.60 eV for local, Rydberg and CT states, respectively.[52] Nevertheless, the average error tends to reduce when going from LDA to GGA and from GGA to *meta*-GGA, even though the latter still underrate the experimental reference. Indeed, for a set of 49 $\pi \rightarrow \pi^*$ transitions of dyes, we reached[59] a MSE of 0.47 eV with the two most popular GGA (BLYP[69,70] and PBE)[73] but 0.35 eV and 0.29 eV with two *meta*-GGA, VSXC[74] and M06-L,[77] respectively. The same was found by Caricato *et al.* using their 69 states/11 molecules set: VSXC[74] statistically outperformed all tested GGA by *ca.* 0.10 eV irrespective of the consideration of all states or only the lowest-lying ones.[58] Another widely accepted outcome is that RSH tend to correct the errors obtained for CT states.[52,92,105,106] Amongst this family of functional, CAM-B3LYP,[95] ωB97XD[94] and LRC-ωPBEh[106] are probably three of the most satisfying. Indeed, for 614 states of 483 solvated organic molecules, we obtained a MAE of 0.30 eV with the former,[55]

whereas Goerigk and Grimme reported a 0.18 eV average deviations for 12 low-lying excited states obtained on large molecules.[56] Similar conclusions hold for Caricato's set for which the smallest average errors amongst the tested RSH are obtained with CAM-B3LYP[95] (0.23 eV for the first states, 0.33 eV when all states are considered).[58] For the global hybrids, the results are slightly more controversial, or at least, more affected by the answer given to the above-mentioned dilemma. Using the most popular but non-physical scheme consisting in comparing experimental λ_{max} to vertical TD-DFT energies, we concluded that global hybrids incorporating 15–30% of exact exchange are the most efficient with MAE $<$ 0.25 eV for our 614 states benchmark.[55] Caricato and coworkers selected the other tactics (physically-grounded comparisons on small gas-phase molecules) and concluded that two xc functionals including a large share of HF exchange (BMK[89] and M05-2X)[91] are the most satisfying (MAE of 0.36 eV).[58] However, when selecting only the lowest-lying states, the smallest deviations are reached with a 20% hybrid, namely B3P86,[69,71,80] in parts illustrating the impact of Rydberg states in the full set.[58] For the first band of 12 large dyes, Goerigk and Grimme corrected experimental 0–0 values with theoretical estimates of adiabatic-vertical shifts, zero-point energies and solvent effects, so to compare directly "experimental" gas-phase vertical energies to TD-DFT values.[56] With this procedure, they obtained a MAE of 0.31 eV for B3LYP,[80,81] but 0.19 eV for BMK,[89] hinting that a larger share of exact exchange might be necessary when going beyond the vertical approximation. As for Thiel's set of molecules, double-hybrids including perturbative corrections seem to be the closest to chemical accuracy (MAE of 0.16 eV).[56]

To summarise, the expected TD-DFT accuracy is strongly dependent on the nature of the considered state. For low-lying singlet transitions that are the focus of the next sections, the average deviations often remain in the 0.2–0.3 eV range when using typical hybrid functionals, such as B3LYP[80,81] or PBE0,[85,86] an error that could even be decreased when double-hybrids including (*D*) corrections to the transition energies are applied. For states presenting a strong push–pull or Rydberg character, RSH relying on a relatively soft attenuation, *e.g.* CAM-B3LYP[95] and ωB97XD,[94] seems to be balanced compromises as they deliver relatively small deviations for CT states without significantly degrading the accuracy of local states. Of course, some specific cases (significant doubly-excited character or cyanine-like transitions)[53,63,107–109] remain problematic for conventional LR TD-DFT even if low-lying, and errors larger than 0.5 eV are not uncommon for such states.

3 Solvent

TD-DFT approaches are nowadays largely used in combination with models which accounts for the effects of the environment, from now on indicated as solvation models. This coupling represents one of the most effective computational strategies to simulate excitation and deexcitation processes in the condensed phase as well as to reproduce the related spectroscopic data. Several solvation models have been coupled to TD-DFT approaches; here, it is useful to divide them into two main families, the QM/MM and the QM/continuum. In both cases the part of the system which is directly involved in the process of interest, the chromophore(s), is treated quantum-mechanically through TD-DFT while the rest is treated either using classical molecular mechanics (MM) or introducing a continuum dielectric. In the latter case an artificial boundary between the QM and the continuum part has to be introduced, this boundary represents the so-called *cavity surface*. The two approaches even if very different in the way they describe the environment present a fundamental common characteristic. Both of them use a modified (or effective) Hamiltonian in which the vacuum term, $\hat{H}_0$, is combined with a new operator describing the interaction between the classical and the QM part, namely:

$$\hat{H}_{\text{eff}}|\Psi\rangle = (\hat{H}_0 + \hat{V}_{\text{QM/Class}})|\Psi\rangle = E|\Psi\rangle \quad (1)$$

In most QM/MM approaches this additional operator is represented in terms of an electrostatic interaction between the point charges which represent the solvent atoms and the QM charge distribution. When a polarisable MM approach is used, a further term has to be considered representing the interaction between the QM part and, for example, the induced dipoles of the solvent.

When a continuum approach is used, different formulations of the $\hat{V}_{\text{QM/Class}}$ operator are possible. For example in the simplest QM/continuum formulations based on the Onsager formulation of the continuum models,[110] this operator is represented by a dipole operator scaled by a factor which depends on the solvent permittivity and the cavity radius (in these models in fact the solute–solvent boundary is a spherical surface). In the most recent and most refined models where the cavity used follows the 3D structure of the QM system, it is not possible to obtain an analytical formulation of $\hat{V}_{\text{QM/Class}}$ as for the spherical case and thus more complex formulations are necessary. One of the most used formulations is based on the concept of *apparent surface charge*, ASC. Within this formalism the electrostatic interaction between the QM system and the solvent can be represented in terms of an ASC distribution spreading on the cavity surface which completely describes the polarisation of the dielectric. In the computational implementation of the model, the ASC is often described in terms of a set of point-like charges placed on the representative points of the mesh used to represent the cavity surface. Among ASC models, the Polarisable Continuum Model (PCM) approach[28] is one of the most used: PCM nowadays represents a family of continuum models which differentiate one from the other in terms of the definition of the ASC and the way it is numerically represented.

The extension of QM/MM and QM/continuum models to excited state QM methods and in particularly TD-DFT has been made available since various years and thus the relative literature is quite vast. The interested reader can find a useful tool to enter into this field and/or to deepen their theoretical and computational aspects in recent reviews,[111,112] here we shall analyse selected aspects common to both approaches and report some examples.

The first important common aspect that is important to recall here is that when fast processes are considered, such as vertical excitations both in absorption and in emission, the solvent polarisation can be characterised, entirely or in part,

by response times which are longer than those involved in the fast process. In these cases, possible *nonequilibrium* effects can play a role.[27] In particular, in polar solvents, the *nonequilibrium* solvation is significantly different from the equilibrium one as only the minor electronic part of its polarisation immediately rearranges in the new configuration corresponding to the new electronic state while the major inertial, or orientational, part is generally too slow and lags behind, remaining in the configuration of the initial state. To quantify the relative contributions of the two parts of the polarisation we recall that for a polar solvent the electronic polarisation is determined by a dielectric constant (generally called *optical permittivity*) of the order of the square of the refractive index, *i.e.* around 2, whereas the complete permittivity typically exceeds 20. Nonequilibrium effects can be properly taken into account in PCM-like approaches by simply partitioning the ASC charges into two sets representing the electronic and the inertial component of the total polarisation, respectively, and treating them with different response behaviors. Also QM/MM approaches take into account nonequilibrium effects; as a matter of fact by using charges that do not change in the fast process they automatically describe the inertial part of the solvent response. However, in order to include the electronic component they have to be polarisable.

The second important aspect to recall is of QM origin, and it is related to the use of an effective Hamiltonian which introduces a new theoretical aspect in the extension of solvation models to the TD-DFT formulation. If the solvent-induced operator in the effective Hamiltonian explicitly depends on the electronic density of the state of interest (such as with a polarisable MM or using a PCM like description) its extension to the TD-DFT description (or to a similar LR method) is not unequivocal. In fact, different approximations can be introduced starting from the simplest one in which the effect of the solvent is present only in the reference ground state but it does not explicitly enter in the TD-DFT response equations. This zero-order approximation can be improved by introducing an explicit LR solvent-induced contribution to the response equations. Such a term corresponds to the interaction energy between the transition density and the solvent polarization due to the transition density itself. However, this type of response differs from the one that would be obtained if excited state densities were available, as in this latter case the interaction would be between the state density and the corresponding state-specific (SS) solvent response. As a result, the solvent effects calculated with LR methods are intrinsically different from those obtained with wave-function based approaches such as CI, MCSCF, CASSCF....[113,114] Starting from the proposal by Caricato *et al.*, known as corrected LR (cLR),[30] some strategies have been made available to recover the proper SS solvent polarisation within a TD-DFT/PCM framework.[115] The main advantage of these schemes is that they allow to recover a more physically correct description of the solvent response while keeping the efficiency and easiness of TD-DFT.

In practice, one notices significant qualitative and quantitative variations of the estimated transition energies when solvent effects are accounted for, and the differences between the *nonequilibrium* and *equilibrium* models are non-negligible.

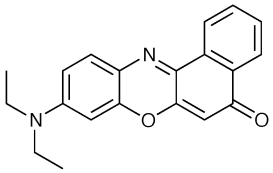

Fig. 3 Chemical structure of Nile Red.

For instance, for eight typical anthraquinoidic dyes solvated in methanol, we obtained an average difference between the gas-phase and LR-PCM (*nonequilibrium*) vertical TD-DFT values of −0.13 eV, but the individual variations varies from −0.02 eV to −0.30 eV, depending on the substituents.[116] For comparison, the average shift computed with the LR-PCM (*equilibrium*) approach attains −0.23 eV whereas the indirect solvent effect (that is the variations of transition energies due to the modification of the ground-state geometrical parameter) does not exceed −0.03 eV for the same set.[116] However, it should be noted that, for low-lying $n \rightarrow \pi^*$ excited-states, the discrepancies between the *nonequilibrium* and *equilibrium* models are apparently smaller, *e.g.* 0.02 eV for formaldehyde,[117] though the solvent effects tend to be more significant than for their $\pi \rightarrow \pi^*$ counterparts.[118] cLR solvent shifts are also significantly different from LR shifts. This can be illustrated by a comparison of the gas-phase and PCM (*n*-heptane) absorption and emission energies of Nile Red (Fig. 3), a well-known organic dye.[119] With B3LYP (CAM-B3LYP), we computed a variation of −0.16 eV (−0.18 eV) for the absorption using the LR-PCM approach, but −0.07 eV (−0.08 eV) with the corresponding cLR scheme, a difference of a factor of two. For the emission, the LR figures are −0.15 eV (−0.18 eV) whereas their cLR counterparts are −0.04 eV (−0.05 eV), indicating that only the latter models can be considered as reasonable. On the contrary, for coumarin C153, the LR solvatochromic shifts computed for vertical transitions are smaller than the results obtained with more refined approaches.[31]

Moving to QM/MM models, the applications to TD-DFT have been increased a lot in the last few years, most of them refer to systems in standard solvents but examples concerning less uniform and homogeneous environments are more interesting. It is in fact in these cases that possible significant differences between the two descriptions of the environment (the continuum and the atomistic) appear: a specific example will be reported in the next section. Of course, QM/QM partitioning models may also be applied to investigate solvent effects or large interacting molecules. In this field, previous applications of the fragment molecular orbital (FMO) approach to TD-DFT have been proposed, either alone,[120] or together with a PCM model.[121] To finish this section,we have also to mention the so-called embedded DFT approach that constitutes a reasonable alternative to quickly estimate solvatochromic shifts.[122,123]

4 Complex environments

4.1 Cage-dye

Simulating the spectra of chromophores in a less uniform environment remains a significant challenge. Of course, some cases are suited for standard TD-DFT calculations, such

as hydrogen-bonded DNA bases[124,125] or dyes surrounded by a small explicit well-defined hydration shell, for which combining explicit and implicit solvent models is an adequate strategy.[27,126] When only hybrid QM/MM schemes may provide a valid representation of the treated case, simulations become more complex. A major challenge is to account for the response of the MM part to the variation of electronic densities implied by photon absorption in the QM chromophore-containing domain (see discussion of *non-equilibrium* in the previous section). Several strategies have been designed and applied[127–141] (see also FMO in the previous section), and we limit our presentation to one specific tutorial example here. The following sections provide extra examples of hybrid multi-level schemes.

The example we wish to discuss is the modelling of a squaraine dye encaged inside a tetralactam macrocycle (see Fig. 4).[138] This structure has been synthesised by the group of Smith,[142] aiming at providing a host efficiently protecting the sensitive chromogen from chemical attacks but not affecting significantly its optical properties. Consequently, the experimental variation of the λ_{max} is limited to a tiny value of −0.06 eV,[142] a small effect representing a significant challenge for TD-DFT. A TD-PBE0/6-31++G(d,p)//PBE0/6-31G(d,p) calculation is able to correctly restore this bathochromic shift (−0.07 eV) but at the price of extreme computational resources.[138] As expected, the frontier orbitals implied in the visible transition of interest are purely localised on the central dye (Fig. 5) and this finding, together with the lack of covalent bonds between the squaraine and its host, provides an ideal prototype case for TD-DFT/MM models. In a first approach, "only" the ground-state polarisation has been considered, by self-consistently calculating the atomic point charges of the cage polarising the QM part (so-called SCPC, *self-consistent point charges* procedure in ref. 138) and this provided a qualitatively incorrect +0.10 eV estimate for the cage impact. In a second approach the response of the tetralactams electronic density to the excited-state electronic distribution of the dye has been modelled through a *nonequilibrium* polarisable dielectric continuum,[28] but keeping the SCPC MM point charges of the cage (ERS, *electronic response of the surroundings* approach in ref. 138). In this a way, the estimated shift was −0.09 eV, in good agreement with the full TD-DFT estimates (as well as with experiment), but for a computational cost reduced by nearly two orders of magnitude compared to the QM-only calculation.

4.2 Metal-dye

A molecule in the vicinity of a metal surface or a metal nanoparticle (MNP) can exhibit very different optical properties from an isolated molecule.[143–148] From the theoretical point of view, different research groups have tried to model these metal-induced changes in molecular properties, and to simulate the related spectroscopies, especially surface-enhanced Raman scattering (SERS), but also metal-enhanced fluorescence (MEF or also known as SEF, surface-enhanced fluorescence) (see the recent review by Morton *et al.*,[149] and references therein). For MEF, it is now widely recognised that metal NPs generally enhance the radiative decay rates of fluorophores as well as the initial process of electronic absorption. Additionally, metal NPs also activate a new nonradiative channel of decay through excitation energy transfer from the fluorophore to the NPs, explaining the sometimes very strong fluorescence quenching observed experimentally. Therefore, a global enhancement of a fluorescent system is the result of a competition between local enhancement and quenching. All these effects result from interactions of the excited-state fluorophores with the collective oscillations of conduction electrons in the metal NPs that result in the so-called localised surface plasmon resonance (LSPR).

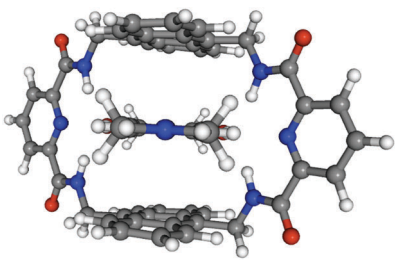

Fig. 4 Side view of the squaraine-tetralactam complex of ref. 142.

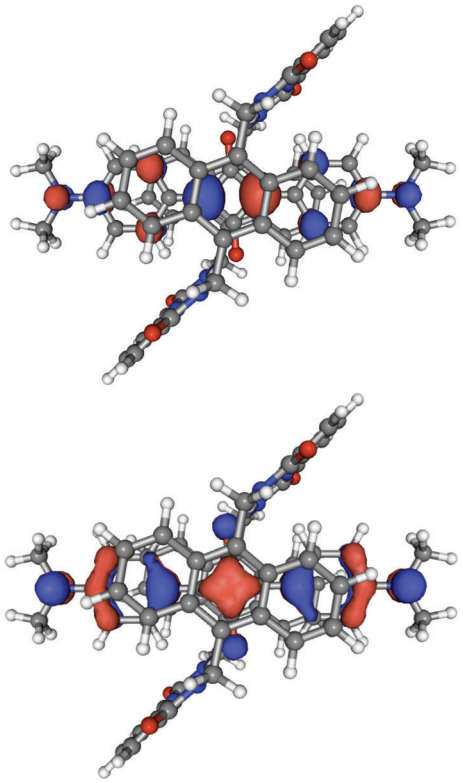

Fig. 5 HOMO (bottom) and LUMO (top) of the system represented in Fig. 4.

Classical electrodynamics methods provide an accurate and efficient simulation of optical properties of MNPs. Several numerical simulation methods, such as Mie theory,[150] discrete dipole approximation (DDA),[151] and finite difference time domain (FDTD),[152] exist and have been widely used to model different geometrical nanostructures. When moving to the simulation of the metal-enhancement of the molecular response properties or spectroscopic signals of nearby molecules, electronic structure methods become of fundamental importance in the understanding and the rationalisation of experimental

findings and prediction and design of novel nanostructured materials with specific optical properties. Within this framework, a very effective approach is that given by TD-DFT either coupled to continuum or discrete (MM) descriptions of the MNPs. As regards MEF, however, the applications of accurate QM descriptions are still quite limited as most studies use either a point dipole approximation or a two-level system when modelling the molecule. An example of QM extended descriptions is represented by the combination of a PCM-like description of the metal and a TD-DFT description for the molecule electronic transition process and the resulting fluorescence signal.[153–155] Using such an approach, the global effect of the MNPs (and possibly a solvent) on the fluorescence of a given molecular system is obtained by calculating the so-called relative brightness, Φ^{RB}, that is, the quantity more directly related to experiments dealing with MEF as it quantifies metal-induced enhancement or quenching of the fluorescence at a constant excitation intensity,

$$\Phi^{RB} = f_{abs}\Phi_{QY} = f_{abs}\frac{\Gamma^{rad}}{\Gamma^{rad} + \Gamma^{nonrad}} \qquad (2)$$

where the factor f_{abs} takes into account the different population in the fluorophore excited state induced by the metal influence on the molecular absorption and Φ_{QY} is the fluorescence quantum yield. All the involved quantities, f_{abs}, the radiative (Γ^{rad}), and the nonradiative (Γ^{nonrad}) decay rates, are obtained quantum-mechanically by explicitly including mutual polarisation effects among all the components (fluorophore and NPs, fluorophore and solvent, NPs and solvent, and NPs among themselves when an array is considered).[156] Within such a framework, the interaction between the molecule and the composite environment (metal and solvent) is electrostatic in nature, and it is due to the mutual polarisation. The polarisation of the environment is accounted for within the PCM approach described in the previous section, namely using ASC on the surfaces of (i) the molecular cavity embedding the solvated fluorophore and (ii) the metal particle(s) (see Fig. 6 for a graphical example of a possible molecule-MNP array).

The electronic excitation energies and transition densities of the fluorophore are calculated within the TD-DFT approach even if a semiempirical CIS method using Zerner's intermediate neglect of differential overlap (ZINDO) has been used as well.[157] When solving the TD-DFT/PCM equations, the transition energies and transition densities obtained take into account the polarisation effects of the environment (MNPs + solvent) and they can be used to obtain the quantities requested in eqn (2). In particular, both f and Γ^{rad} can be obtained by calculating the effective transition dipole which is the sum of the molecular transition dipole and the dipoles induced on the metal and the solvent by the molecular transition. In the PCM approach, these two induced terms are calculated in terms of the corresponding induced charges on the surface of the metal cavity and the molecular cavity, respectively. To obtain the nonradiative decay rate, the imaginary part of the complex eigenvalues of the TD-DFT equations in the presence of the interaction of the transition density with the oscillating metal polarisation induced by the transition density itself. Such an imaginary component is originated by the complex nature of the frequency dependent dielectric permittivity of the metal, which determines such induced charges. Usually, to describe the response of the MNPs, in the PCM calculations a local, frequency-dependent permittivity taken from experimental data (and corrected for the limited mean free-path according to the Drude model) is used.

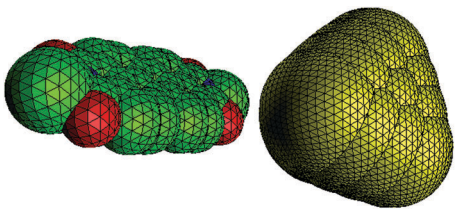

Fig. 6 PCM representation of a fluorophore nearby a pyramid metal nanoparticle.

This approach has been used to understand how the MNP size, shape and composition differentially affect the fluorescence signal of different fluorophores, as well to describe the role of the solvent and of the coupling of its polarisation with that of the MNPs, and finally to analyse the effects of the couplings among different MNPs. For example, a recent application[156] of such an approach to the study of the fluorescence intensity of a dye (naphthalenemonoimide) positioned within a four-silver nanoparticle square array has shown that the number and the location of hot spots in which fluorescence enhancement is observed are strictly related to solvent-induced effects both on the optical properties of the fluorophore and the MNP and on the plasmon couplings among the MNPs. In particular, by comparing such a combined QM/continuum description with a parallel one using a TD-DFT description for both the fluorophore and the metal particles, conditions for the presence or absence of additive behaviors in the MNP array have been revealed: when plasmon couplings are negligible, additivity is present in the nonradiative component of the fluorophore decay, and this can be exploited to predict the position and the number of fluorescence hot spots in extended MNP monolayers by studying single-particle systems.

Recently, other hybrid QM/classical models have appeared,[158,159] showing that the research in this field is very active and that the coupling between QM (and especially TD-DFT) approaches with classical descriptions of the metal nanoparticles represents a very promising strategy to approach these multiscale problems.

4.3 Surface-dye

The handling of excited electronic state features for technological applications often requires the grafting of molecules (*i.e.* the photoactive element) over a surface. A strong interaction with the surface, such as chemisorption, is often required to ensure a sufficiently long lifetime of the device but it can significantly alter both structural and electronic features of the dye molecule and, as consequence, its optical properties. As an illustrative example, the modeling of dye properties in dye-sensitized solar cells (DSSC) has been chosen. In these devices, the optical response of a large band

gap semiconductor (as TiO_2 or ZnO) is shifted from the UV to the visible region by dye sensitization (see ref. 160 for instance for a more detailed description of DSSC operating principles). Among the large amount of dyes tested, ruthenium polypyridyl complexes, such as *cis*-[Ru(4,4′-COOH-2,2′-bpy)$_2$(NCS)$_2$], the so-called N3 dye, still represent the reference in terms of light-to-energy conversion efficiency.[161] For such a reason, the UV-Vis spectra of N3 derivatives have been analyzed in detail in several experimental and theoretical studies.[162–166] Basically, these compounds are characterized by two absorption bands, centered at *ca.* 400 nm and 540 nm.[165,166] Experimentally it is also known that the absorption spectrum shows negligible variations when going from the free (*i.e.* N3 in solution) to the adsorbed dye (*i.e.* N3 on TiO_2). To assess this point theoretically, the UV-Vis spectrum of N3 was first computed at the TD-PBE0 level of theory for the isolated N3 and the adsorbed N3 in the gas phase (that is in the absence of solvation effects). The latter system is represented by N3 absorbed over a slab of TiO_2 obtained from full 3D calculations, for a cluster containing in total 986 atoms (see Fig. 7).[167] A QM//QM′ electronic embedding model,[168,169] based on the ONIOM scheme,[170] has been considered to model the surface effects on the UV-Vis absorption spectrum. This model has been successfully used to model dye properties in another DSSC system, namely eosin-Y on a ZnO surface.[169] In this approach, the high computational level is obtained using the PBE0 functional while the low-level is represented by the SVWN exchange-correlation functional. The Mulliken charges of the real-system low-level are used to define the embedding potential to be used in the TD-DFT Hamiltonian. The model system is represented by the N3 molecule, while the real system, including the N3 molecule, is defined by the above-mentioned cluster.

In agreement with the experimental findings, adsorption on the surface does not alter the features of the spectra, both in terms of transition energies and intensities. In particular, in both cases two distinct bands are computed with a negligible shift in the absorption maxima upon adsorption of the dye on the semiconductor surface (see Fig. 8). Nevertheless, from a quantitative point of view, the two bands are predicted with different accuracy. While the transition at higher energy is quantitatively reproduced (that is computed at *ca.* 395 *versus* the 402 nm of the experimental spectra), the band at lower energy is predicted significantly red-shifted with a computed maximum at *ca.* 694 nm with respect to the 544 nm experimentally observed.[166] This error is significantly larger than the expected error for similar types of transition at the level of theory used (see Section 2).[162,171] In fact, both bands

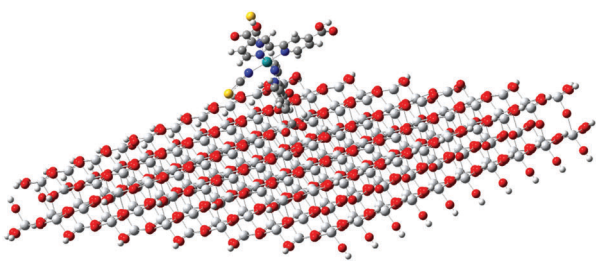

Fig. 7 Sketch of the 986-atom cluster used for UV-Vis spectra simulations of N3/TiO_2 assembly.

are dominated by Metal-to-Ligand-Charge-Transfer (MLCT) transitions, corresponding to a single excitation from a d orbital of the metal to a π* orbital of the ligand. In particular, the lowest band corresponds to a HOMO–LUMO excitation, while the higher band mainly involves a lower energy d orbital (the HOMO − 2) and a higher energy empty π* orbital (the LUMO + 2). The latter is a compact π* orbital localized on only one ring of each bipyridyl ligand.[164]

Clearly, since the virtual π* orbitals (especially the LUMO) are significantly affected by the presence of a solvent (being more polarizable and exposed to it) while the d orbitals of the metal are localized on the Ru core, and thus not sensitive to the presence of a solvent, significant solvatochromic effects are expected when going from the gas-phase to solution. This is indeed what is found in the case of the isolated system whose spectrum computed in water (represented by a continuum model) shows a first transition significantly blue-shifted with respect to gas phase results (towards the experimental value of 544 nm). The higher energy transitions contributing to the second band are, on the other hand, less affected by the presence of the solvent, consistent with the less polarizable (hard) nature of the orbitals involved. Since no significant variation between the gas-phase spectra of the isolated and adsorbed N3 dye is found, the same should hold also for the solvated system. Indeed when the continuum model is added to the cluster within a QM//QM′//PCM approach, the spectrum for the N3 system adsorbed on the surface and in the presence of a solvent is very similar to that computed for the isolated N3 in solution. This behavior is, indeed, also experimentally observed.

5 Interacting excitations: EET

The nonradiative process of EET from a photoexcited system, the donor, to a proximate ground-state system, the acceptor, is of fundamental interest in many different fields ranging from biosciences to nanotechnology[172–174] where EET is at the basis of many devices such as the fluorescence-based sensors, organic light-emitting diodes or artificial light-harvesting devices. The fundamental theory relating experimental observables to the

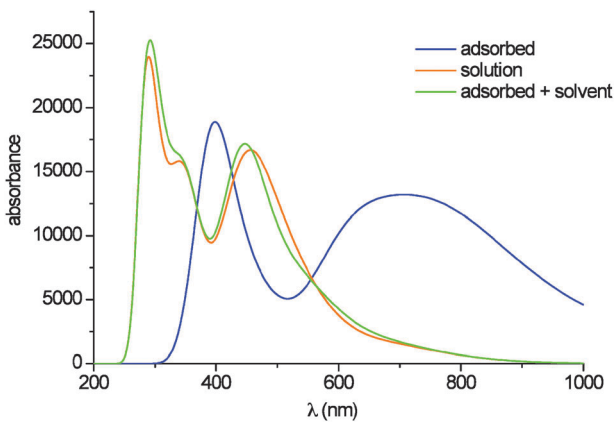

Fig. 8 UV-Vis absorption spectra of the N3 dye in different environments. All spectra have been simulated by associating a single Gaussian function with a half-height width of 0.15 eV to each computed transition.

mechanism of EET was due to Förster who described the process within a dipole–dipole approximation of Coulomb interactions between donor and acceptor excitations.[175] The Förster theory was successively supplemented with the so-called Dexter formulation[176] accounting for higher multipolar terms and for exchange effects and subsequently applicable to cases in which EET involves forbidden transitions (null dipole–dipole interactions).

In the last few years, many QM based approaches have been proposed to improve these older formulations. Among the most effective proposals there are those based on TD-DFT descriptions of the excitations. TD-DFT equations in fact can be used to obtain the transition densities necessary to calculate the electronic coupling determining the EET rate.[177–179] For instance, TD-DFT descriptions have been combined with the so-called *transition density cube* (TDC) method, which numerically calculates the coulombic interaction between transition densities obtained from *ab initio* methods by representing them in three-dimensional grids or *cubes*.[180] More recently a similar, though more general approach, based on an extension of TD-DFT description for interacting systems, has been proposed.[177,178] As for TDC, transition densities are used to evaluate the coupling but now also exchange and correlation effects can be taken into account together with the effects of the surroundings.

The environment plays in fact a fundamental role in determining the efficiency of the EET process, because it modulates the electronic interactions promoting it as well as the energies of the interacting electronic states thus providing the resonance conditions necessary for the transfer reaction. As already pointed out by Förster in the formulation of his coulombic model, the presence of an environment introduces a screening in the donor/acceptor interactions and thus a reduction of the coupling. Such a screening effect was introduced by Förster through a scaling factor equal to the inverse of the square of the solvent refractive index, $1/n^2$. The recent extensions within the TD-DFT formalism however go beyond such an approximation by including the effects of the environment both in the calculation of the transition properties of donor and acceptor systems as well in their electronic (or excitonic) coupling.[181] Within this framework, PCM has been originally adopted to describe the environment[182] whereas more recently an extension to a polarisable MM description has been presented.[183] It is in fact the polarisable part of the environment response which allows for the screening effect which means that non-polarisable MM approaches are not well suited to properly describe the effect of the environment in EET. It has been shown that QM/MM and PCM results for the environmental screening are very similar when an averaged picture is sufficient. However, when the specific influence of an heterogeneous medium as present in proteins plays a role, the QM/MM approach is obviously to be preferred since it keeps the atomistic nature of the different components of the environment.[184]

An alternative TD-DFT approach aimed at the calculation of the excitonic coupling has been proposed within the subsystem formulation of density functional theory known as the frozen-density embedding (FDE) method.[185] More recently the method has been extended to include screening effects of the solvent and compared with the polarisable QM/MM approach. A good overall agreement in the description of the solvent screening has been found with deviations only for the effect of the closest solvent molecules, whereas the screening introduced by outer solvation shells is alike in both schemes.[186]

All these recent examples of combination of TD-DFT with models aiming at describing the electronic coupling in EET complexes have clearly demonstrated the strong limitations of the simplified dipole approximation as well as they have unraveled unprecedented insights on how environment screening effects modulate EET.

Clearly, much more remain to be done to clarify the open problems in the field and TD-DFT approaches surely represent one of the most cost-effective strategies. However, also for EET-related quantities, namely transition energies, densities and dipoles, and electronic couplings, the well-known problems of TD-DFT xc functionals can represent an important weakness. Few years ago a comparative study on the influence of the QM method including the basis set on the evaluation EET properties for a series of chromophores and the corresponding donor–acceptor pairs typically found in organic electrooptical devices and photosynthetic systems was performed using five different QM levels of description (ZINDO, CIS, TD-DFT, CAS-SCF, and SAC-CI).[187] As expected, excitation energies were found to vary strongly with the QM method. In contrast, transition dipole moments showed to be much less sensitive to the particular level of theory, and even less with respect to the basis set. Moving to electronic couplings, their values were found to be more stable than the excitation energies with respect to the QM level of description and to have little dependence on the basis set. However, TD-B3LYP led to couplings reduced by more than 20% with respect to SAC-CI. In addition, it was found that when using TD-DFT methods, a possible mixing of the state of interest with spurious low-lying states can introduce strong variations in the electronic coupling. This problem is expected to be largely alleviated by more recent developments of long-range corrected exchange-correlation functionals but this remains to be investigated.

6 Summary

In this perspective, we have reviewed several schemes that have been recently developed to account for environmental effects during TD-DFT calculations. From a quantitative point of view, the expected accuracy of TD-DFT is *ca.* 0.2–0.3 eV, once modern hybrid functionals are applied, but such an accuracy can only pertain when a physically-sound description of the surroundings of the chromogen is used. In that framework, the response of the environment to the excited-state of the considered chromophore has to be modelled adequately, as it induces not only significant shifts, but may also tune the nature of the intrinsic phenomenon. For bulk solvent effects, the latest (state-specific) approach of the PCM model allows for accurate evaluation of solvatochromic shifts for both absorption and fluorescence, with corrections with respect to the standard linear-response results that are often non-negligible. More complex cases, *e.g.* host–guest interactions,

dye in the vicinity of a metal or grafted on a semi-conducting surface, may be considered using hybrid QM//MM, QM//QM′ or QM//PCM models, allowing to understand the impact of a protecting cage, to optimize the properties of DSSC, to mimic MEF and SERS spectroscopies as well as to simulate nonradiative electronic energy transfer.

Though it is crystal-clear that further developments are required in the fundamental aspects of TD-DFT (beyond LR response), selected functionals (more robust functionals applicable to all type of states) and environment (less "crude" approximations), this perspective illustrates that reasonable tools are already available to treat a wide variety of complex situations.

Acknowledgements

D. J. thanks *Région des Pays de la Loire* for financial support in the framework of a *recrutement sur poste stratégique*. The COST-CMTS Action CM1002: COnvergent Distributed Environment for Computational Spectroscopy (CODECS) and its members are acknowledged.

References

1 E. Runge and E. K. U. Gross, *Phys. Rev. Lett.*, 1984, **52**, 997–1000.
2 M. E. Casida, in *Time-Dependent Density-Functional Response Theory for Molecules*, ed. D. P. Chong, World Scientific, Singapore, 1995, vol. 1, pp. 155–192.
3 R. E. Stratmann, G. E. Scuseria and M. J. Frisch, *J. Chem. Phys.*, 1998, **109**, 8218–8224.
4 A. Dreuw and M. Head-Gordon, *Chem. Rev.*, 2005, **105**, 4009–4037.
5 A *TD-DFT or TDDFT or Time-Dependent Density Functional Theory* search provided 100, 181, 333, 550, 670 and 825 publications for 2000, 2002, 2004, 2006, 2008 and 2010, respectively.
6 A. D. Bacon and M. C. Zerner, *Theor. Chim. Acta*, 1979, **53**, 21–54.
7 J. J. P. Stewart, *MOPAC2002*, Fujitsu Ltd., Tokyo, Japan, 2001.
8 J. Fabian, *Theor. Chem. Acc.*, 2001, **106**, 199–217.
9 M. Caricato, B. Mennucci and J. Tomasi, *J. Phys. Chem. A*, 2004, **108**, 6248–6256.
10 D. Jacquemin and E. A. Perpète, *Chem. Phys. Lett.*, 2006, **429**, 147–152.
11 M. Matsuura, H. Sato, W. Sotoyama, A. Takahashi and M. Sakurai, *J. Mol. Struct. (THEOCHEM)*, 2008, **860**, 119–127.
12 M. R. Silva-Junior and W. Thiel, *J. Chem. Theor. Comput.*, 2010, **6**, 1546–1564.
13 L. Serrano-Andrès and B. O. Roos, *Chem.–Eur. J.*, 1997, **3**, 717–725.
14 J. Fabian, L. A. Diaz, G. Seifert and T. Niehaus, *J. Mol. Struct. (THEOCHEM)*, 2002, **594**, 41–53.
15 M. Parac and S. Grimme, *J. Phys. Chem. A*, 2002, **106**, 6844–6850.
16 M. van Faasen and P. L. Boeij, *J. Chem. Phys.*, 2004, **120**, 8353–8363.
17 L. Blancafort and A. A. Voityuk, *J. Phys. Chem. A*, 2007, **111**, 4714–4719.
18 A. L. Sobolewski, D. Shemesh and W. Domcke, *J. Phys. Chem. A*, 2009, **113**, 542–550.
19 D. Shemesh, A. L. Sobolewski and W. Domcke, *J. Am. Chem. Soc.*, 2009, **131**, 1374–1375.
20 M. J. G. Peach, C. R. Le Sueur, K. Ruud, M. Guillaume and D. J. Tozer, *Phys. Chem. Chem. Phys.*, 2009, **11**, 4465–4470.
21 A. D. Quartarolo, E. Sicilia and N. Russo, *J. Chem. Theor. Comput.*, 2009, **5**, 1849–1857.
22 A. D. Quartarolo and N. Russo, *J. Chem. Theor. Comput.*, 2011, **7**, 1073–1081.
23 A. M. Losa, I. F. Galvan, M. A. Aguilar and M. E. Martin, *J. Phys. Chem. B*, 2007, **111**, 9864–9870.
24 M. Caricato, B. Mennucci, G. Scalmani, G. W. Trucks and M. J. Frisch, *J. Chem. Phys.*, 2010, 084102.
25 M. Caricato, T. Verven, G. W. Trucks and M. J. Frisch, *J. Chem. Theor. Comput.*, 2011, **7**, 180–187.
26 K. Sneskov, T. Schwabe, J. Kongsted and O. Christiansen, *J. Chem. Phys.*, 2011, **134**, 104108.
27 M. Cossi and V. Barone, *J. Chem. Phys.*, 2001, **115**, 4708–4717.
28 J. Tomasi, B. Mennucci and R. Cammi, *Chem. Rev.*, 2005, **105**, 2999–3094.
29 G. Scalmani, M. J. Frisch, B. Mennucci, J. Tomasi, R. Cammi and V. Barone, *J. Chem. Phys.*, 2006, **124**, 094107.
30 M. Caricato, J. Mennucci, B. Tomasi, F. Ingrosso, R. Cammi, S. Corni and G. Scalmani, *J. Chem. Phys.*, 2006, **124**, 124520.
31 R. Improta, V. Barone, G. Scalmani and M. J. Frisch, *J. Chem. Phys.*, 2006, **125**, 054103.
32 V. Barone, J. Bloino, S. Monti, A. Pedone and G. Prampolini, *Phys. Chem. Chem. Phys.*, 2011, **13**, 2160–2166.
33 A. Savin, in *Recent Developments and Applications of Modern Density Functional Theory*, ed. J. M. Seminario, Elsevier, Amsterdam, 1996, ch. 9, pp. 327–354.
34 H. Iikura, T. Tsuneda, T. Yanai and K. Hirao, *J. Chem. Phys.*, 2001, **115**, 3540–3544.
35 J. Toulouse, F. Colonna and A. Savin, *Phys. Rev. A: At., Mol., Opt. Phys.*, 2004, **70**, 062505.
36 O. A. Vydrov and G. E. Scuseria, *J. Chem. Phys.*, 2006, **125**, 234109.
37 E. Livshits and R. Baer, *Phys. Chem. Chem. Phys.*, 2007, **9**, 2932–2941.
38 J. P. Perdew, A. Ruzsinsky, J. Tao, V. N. Staroverov, G. E. Scuseria and G. I. Csonka, *J. Chem. Phys.*, 2005, **123**, 062201.
39 V. Barone and A. Polimeno, *Chem. Soc. Rev.*, 2007, **36**, 1724–1731.
40 V. Barone, R. Improta and N. Rega, *Acc. Chem. Res.*, 2008, **41**, 605–616.
41 F. Neese, *Coord. Chem. Rev.*, 2009, **253**, 526–563.
42 D. Jacquemin, E. A. Perpète, I. Ciofini and C. Adamo, *Acc. Chem. Res.*, 2009, **42**, 326–334.
43 M. E. Casida, *J. Mol. Struct. (THEOCHEM)*, 2009, **914**, 3–18.
44 M. van Faasen and K. Burke, *Phys. Chem. Chem. Phys.*, 2009, **11**, 4437–4450.
45 N. A. Besley and F. A. Asmuruf, *Phys. Chem. Chem. Phys.*, 2010, **12**, 12024–12039.
46 R. Baer, E. Livshits and U. Salzner, *Ann. Rev. Phys. Chem.*, 2010, **61**, 85–109.
47 M. E. Casida, D. Jacquemin and H. Chermette, *J. Mol. Struct. (THEOCHEM)*, 2009, **914**, 1–2.
48 A. Rubio and A. Marquez, *Phys. Chem. Chem. Phys.*, 2009, **11**, 4436–4436.
49 F. Furche and R. Ahlrichs, *J. Chem. Phys.*, 2002, **117**, 7433–7447.
50 M. Dierksen and S. Grimme, *J. Phys. Chem. A*, 2004, **108**, 10225–10237.
51 D. Jacquemin, E. A. Perpète, G. Scalmani, M. J. Frisch, R. Kobayashi and C. Adamo, *J. Chem. Phys.*, 2007, **126**, 144105.
52 M. J. G. Peach, P. Benfield, T. Helgaker and D. J. Tozer, *J. Chem. Phys.*, 2008, **128**, 044118.
53 M. R. Silva-Junior, M. Schreiber, S. P. A. Sauer and W. Thiel, *J. Chem. Phys.*, 2008, **129**, 104103.
54 L. Goerigk, J. Moellmann and S. Grimme, *Phys. Chem. Chem. Phys.*, 2009, **11**, 4611–4620.
55 D. Jacquemin, V. Wathelet, E. A. Perpète and C. Adamo, *J. Chem. Theor. Comput.*, 2009, **5**, 2420–2435.
56 L. Goerigk and S. Grimme, *J. Chem. Phys.*, 2010, **132**, 184103.
57 D. Jacquemin, E. A. Perpète, I. Ciofini and C. Adamo, *J. Chem. Theor. Comput.*, 2010, **6**, 1532–1537.
58 M. Caricato, G. W. Trucks, M. J. Frisch and K. B. Wiberg, *J. Chem. Theor. Comput.*, 2010, **6**, 370–383.
59 D. Jacquemin, E. A. Perpète, I. Ciofini, C. Adamo, R. Valero, Y. Zhao and D. G. Truhlar, *J. Chem. Theor. Comput.*, 2010, **6**, 2071–2085.
60 M. R. Silva-Junior, M. Schreiber, S. P. A. Sauer and W. Thiel, *J. Chem. Phys.*, 2010, **133**, 174318.
61 D. Jacquemin, E. A. Perpète, I. Ciofini and C. Adamo, *Theor. Chem. Acc.*, 2011, **128**, 127–136.

62 M. Caricato, G. W. Trucks, M. J. Frisch and K. B. Wiberg, *J. Chem. Theor. Comput.*, 2011, **7**, 456–466.
63 M. Huix-Rotllant, A. Ipatov, A. Rubio and M. E. Casida, *Chem. Phys.*, 2011, DOI: 10.1016/J.chemphys.2011.03.019.
64 M. Schreiber, M. R. Silva-Junior, S. P. A. Sauer and W. Thiel, *J. Chem. Phys.*, 2008, **128**, 134110.
65 M. R. Silva-Junior, S. P. A. Sauer, M. Schreiber and W. Thiel, *Mol. Phys.*, 2010, **108**, 453–465.
66 Y. Zhao and D. G. Truhlar, *J. Phys. Chem. A*, 2006, **110**, 5121–5129.
67 J. C. Slater, *Quantum Theory of Molecular ans Solids*, McGraw-Hill, New York, 1974, vol. 4.
68 S. J. Vosko, L. Wilk and M. Nusair, *Can. J. Phys.*, 1980, **58**, 1200–1211.
69 A. D. Becke, *Phys. Rev. A: At., Mol., Opt. Phys.*, 1988, **38**, 3098–3100.
70 C. Lee, W. Yang and R. G. Parr, *Phys. Rev. B: Condens. Matter Mater. Phys.*, 1988, **37**, 785–789.
71 J. P. Perdew, *Phys. Rev. B: Condens. Matter Mater. Phys.*, 1986, **33**, 8822–8824.
72 N. C. Handy and A. J. Cohen, *Mol. Phys.*, 2001, **99**, 403–412.
73 J. P. Perdew, K. Burke and M. Ernzerhof, *Phys. Rev. Lett.*, 1996, **77**, 3865–3868.
74 T. Van Voorhis and G. E. Scuseria, *J. Chem. Phys.*, 1998, **109**, 400–410.
75 A. D. Boese and N. C. Handy, *J. Chem. Phys.*, 2002, **116**, 9559–9569.
76 J. Tao, J. Perdew, V. Staroverov and G. Scuseria, *Phys. Rev. Lett.*, 2003, **91**, 146401.
77 Y. Zhao and D. G. Truhlar, *J. Chem. Phys.*, 2006, **125**, 194101.
78 V. N. Staroverov, G. E. Scuseria, J. Tao and J. P. Perdew, *J. Chem. Phys.*, 2003, **119**, 12129–12137.
79 J. Baker and P. Pulay, *J. Chem. Phys.*, 2002, **117**, 1441–1449.
80 A. D. Becke, *J. Chem. Phys.*, 1993, **98**, 5648–5652.
81 P. J. Stephens, F. J. Devlin, C. F. Chabalowski and M. J. Frisch, *J. Phys. Chem.*, 1994, **98**, 11623–11627.
82 X. Xu and W. A. Goddard III, *Proc. Natl. Acad. Sci. U. S. A.*, 2004, **101**, 2673–2677.
83 H. L. Schmider and A. D. Becke, *J. Chem. Phys.*, 1998, **108**, 9624–9631.
84 C. Adamo and V. Barone, *Chem. Phys. Lett.*, 1997, **274**, 242–250.
85 C. Adamo and V. Barone, *J. Chem. Phys.*, 1999, **110**, 6158–6170.
86 M. Ernzerhof and G. E. Scuseria, *J. Chem. Phys.*, 1999, **110**, 5029–5036.
87 Y. Zhao and D. G. Truhlar, *Theor. Chem. Acc.*, 2008, **120**, 215–241.
88 Y. Zhao, N. E. Schultz and D. G. Truhlar, *J. Chem. Phys.*, 2005, **123**, 161103.
89 A. D. Boese and J. M. L. Martin, *J. Chem. Phys.*, 2004, **121**, 3405–3416.
90 A. D. Becke, *J. Chem. Phys.*, 1993, **98**, 1372–1377.
91 Y. Zhao and D. G. Truhlar, *Acc. Chem. Res.*, 2008, **41**, 157–167.
92 O. A. Vydrov, J. Heyd, V. Krukau and G. E. Scuseria, *J. Chem. Phys.*, 2006, **125**, 074106.
93 J. D. Chai and M. Head-Gordon, *J. Chem. Phys.*, 2008, **128**, 084106.
94 J. D. Chai and M. Head-Gordon, *Phys. Chem. Chem. Phys.*, 2008, **10**, 6615–6620.
95 T. Yanai, D. P. Tew and N. C. Handy, *Chem. Phys. Lett.*, 2004, **393**, 51–56.
96 S. Grimme, *Chem. Phys. Lett.*, 1996, **259**, 128–137.
97 S. Grimme and M. Waletzke, *J. Chem. Phys.*, 1999, **111**, 5645–5655.
98 S. Grimme, *J. Chem. Phys.*, 2006, **124**, 034108.
99 S. Grimme and F. Neese, *J. Chem. Phys.*, 2007, **127**, 154116.
100 M. Head-Gordon, D. Maurice and M. Oumi, *Chem. Phys. Lett.*, 1995, **246**, 114–121.
101 R. J. Cave, F. Zhang, N. T. Maitra and K. Burke, *Chem. Phys. Lett.*, 2004, **389**, 39–42.
102 G. Mazur and R. Wlodarczyk, *J. Comput. Chem.*, 2009, **30**, 811–817.
103 F. Wang and T. Ziegler, *J. Chem. Phys.*, 2004, **121**, 12191–12196.
104 F. Della Sala and E. Fabiano, *Chem. Phys.*, 2011, DOI: 10.1016/J.chemphys.2011.05.020.
105 T. Tawada, T. Tsuneda, S. Yanagisawa, T. Yanai and K. Hirao, *J. Chem. Phys.*, 2004, **120**, 8425–8433.
106 M. A. Rohrdanz, K. M. Martins and J. M. Herbert, *J. Chem. Phys.*, 2009, **130**, 054112.
107 M. Schreiber, V. Bub and M. P. Fülscher, *Phys. Chem. Chem. Phys.*, 2001, **3**, 3906–3912.
108 A. E. Masunov, *Int. J. Quantum Chem.*, 2010, **110**, 3095–3100.
109 R. Send, O. Valsson and C. Filippi, *J. Chem. Theor. Comput.*, 2011, **7**, 444–455.
110 C. Adamo and F. Lelj, *Chem. Phys. Lett.*, 1994, **223**, 54–60.
111 B. Mennucci, C. Cappelli, C. A. Guido, R. Cammi and J. Tomasi, *J. Phys. Chem. A*, 2009, **113**, 3009–3020.
112 H. M. Senn and W. Thiel, *Angew. Chem., Int. Ed.*, 2009, **48**, 1198–1229.
113 R. Cammi, S. Corni, B. Mennucci and J. Tomasi, *J. Chem. Phys.*, 2005, **122**, 104513.
114 S. Corni, R. Cammi, B. Mennucci and J. Tomasi, *J. Chem. Phys.*, 2005, **123**, 134512.
115 R. Improta, G. Scalmani, M. J. Frisch and V. Barone, *J. Chem. Phys.*, 2007, **127**, 074504.
116 D. Jacquemin, J. Preat, M. Charlot, V. Wathelet, J. M. André and E. A. Perpète, *J. Chem. Phys.*, 2004, **121**, 1736–1743.
117 D. Jacquemin, E. A. Perpète, G. Scalmani, M. J. Frisch, I. Ciofini and C. Adamo, *Chem. Phys. Lett.*, 2006, **421**, 272–276.
118 R. Improta and V. Barone, *J. Am. Chem. Soc.*, 2004, **126**, 14320–14321.
119 C. A. Guido, B. Mennucci, D. Jacquemin and C. Adamo, *Phys. Chem. Chem. Phys.*, 2010, **12**, 8016–8023.
120 M. Chiba, D. G. Fedorov and K. Kitaura, *Chem. Phys. Lett.*, 2007, **444**, 346–350.
121 M. Chiba, D. G. Fedorov and K. Kitaura, *J. Comput. Chem.*, 2008, **29**, 2667–2676.
122 J. Kaminsky, S. Gurasov, T. A. Wesolowski and A. Kovalenko, *J. Phys. Chem. A*, 2010, **114**, 6082–6096.
123 X. Zhou, J. Kaminsky and T. A. Wesolowski, *Phys. Chem. Chem. Phys.*, 2011, **13**, 10565–10576.
124 S. Kim and H. F. Schaefer, *J. Phys. Chem. A*, 2007, **111**, 10381–10389.
125 F. Santoro, V. Barone and R. Improta, *J. Comput. Chem.*, 2008, **29**, 957–964.
126 D. Jacquemin, E. A. Perpète, I. Ciofini and C. Adamo, *Theor. Chem. Acc.*, 2008, **120**, 405–410.
127 M. Sugihara, V. Buss, P. Entel, M. Elstner and T. Frauenheim, *Biochemistry*, 2002, **41**, 15259–15266.
128 A.-N. Bondar, S. Fischer, J. Smith, M. Elstner and S. Suhai, *J. Am. Chem. Soc.*, 2004, **126**, 14668–14677.
129 D. Riccardi, P. Schaefer, Y. Yang, H. Yu, N. Ghosh, X. Prat-Resina, P. Konig, G. Li, D. Xu, H. Guo, M. Elstner and Q. Cui, *J. Phys. Chem. B*, 2006, **110**, 6458–6469.
130 M. Hoffmann, M. Wanko, P. Strodel, P. Konig, T. Frauenheim, K. Schulten, W. Thiel, E. Tajkhorshid and M. Elstner, *J. Am. Chem. Soc.*, 2006, **128**, 10808–10818.
131 G. D. Scholes, C. Curutchet, B. Mennucci, R. Cammi and J. Tomasi, *J. Phys. Chem. B*, 2007, **111**, 6978–6982.
132 C. Curutchet, G. D. Scholes, B. Mennucci and R. Cammi, *J. Phys. Chem. B*, 2007, **111**, 13253–13265.
133 T. Mirkovic, A. B. Doust, J. Kim, K. E. Wilk, C. Curutchet, B. Mennucci, R. Cammi, P. M. G. Curmib and G. D. Scholes, *Photochem. Photobiol. Sci.*, 2007, **6**, 964–975.
134 P.-F. Loos, J. Preat, A. D. Laurent, C. Michaux, D. Jacquemin, E. A. Perpète and X. Assfeld, *J. Chem. Theor. Comput.*, 2008, **4**, 637–645.
135 M. Wanko, M. Hoffmann, J. Frähmcke, T. Frauenheim and M. Elstner, *J. Phys. Chem. B*, 2008, **112**, 11468–11478.
136 M. Wanko, M. Hoffmann, T. Frauenheim and M. Elstner, *J. Phys. Chem. B*, 2008, **112**, 11462–11467.
137 M. Caricato, T. Vreven, G. W. Trucks, M. J. Frisch and K. B. Wiberg, *J. Chem. Phys.*, 2009, **131**, 134105.
138 D. Jacquemin, E. A. Perpète, A. D. Laurent, X. Assfeld and C. Adamo, *Phys. Chem. Chem. Phys.*, 2009, **11**, 1258–1262.
139 J. Neugebauer, C. Curutchet, A. Munoz-Losa and B. Mennucci, *J. Chem. Theor. Comput.*, 2010, **6**, 1843–1851.
140 M. Parac, M. Doerr, C. M. Marian and W. Thiel, *J. Comput. Chem.*, 2010, **31**, 90–106.
141 T. Rocha-Rinza, K. Sneskov, O. Christiansen, U. Ryde and J. Kongsted, *Phys. Chem. Chem. Phys.*, 2011, **13**, 1585–1589.

142 J. J. Gassensmith, E. Arunkumar, L. Barr, J. M. Baumes, K. M. DiVittorio, J. R. Johnson, B. C. Noll and B. D. Smith, *J. Am. Chem. Soc.*, 2007, **129**, 15054–15059.
143 H. Metiu, *Prog. Surf. Sci.*, 1984, **17**, 153–320.
144 M. Moskovits, *Rev. Mod. Phys.*, 1985, **57**, 783–826.
145 *Surface-Enhanced Raman Scattering: Physics and Applications*, ed. K. Kneipp, M. Moskovits and H. Kneipp, Springer, Berlin, 2006, vol. 103.
146 K. A. Willets and R. P. van Duyne, *Phys. Chem. Chem. Phys.*, 2007, **58**, 267–297.
147 J. R. Lakowicz, *Anal. Biochem.*, 2005, **337**, 171–194.
148 A. Kinkhabwala, Z. F. Yu, S. H. Fan, Y. Avlasevich, K. Mullen and W. E. Moerner, *Nat. Photonics*, 2009, **3**, 654–657.
149 S. M. Morton, D. W. Silverstein and L. Jensen, *Chem. Rev.*, 2011, **111**, 3962–3994.
150 G. Mie, *Ann. Phys. (Leipzig)*, 1908, **25**, 377–445.
151 W. H. Yang, G. C. Schatz and R. P. van Duyne, *J. Chem. Phys.*, 1995, **103**, 869–875.
152 R. X. Bian, R. C. Dunn, X. S. Xie and P. T. Leung, *Phys. Rev. Lett.*, 1995, **75**, 4772–4775.
153 S. Corni and J. Tomasi, *J. Chem. Phys.*, 2002, **117**, 7266–7278.
154 O. Andreussi, S. Corni, B. Mennucci and J. Tomasi, *J. Chem. Phys.*, 2004, **121**, 10190–10202.
155 S. Vujovic, S. Corni and B. Mennucci, *J. Phys. Chem. C*, 2009, **113**, 121–133.
156 A. Sanchez-Gonzalez, S. Corni and B. Mennucci, *J. Phys. Chem. C*, 2011, **115**, 5450–5460.
157 M. Caricato, O. Andreussi and S. Corni, *J. Phys. Chem. B*, 2006, **110**, 16652–16659.
158 D. J. Masiello and G. C. Schatz, *J. Chem. Phys.*, 2010, **132**, 064102.
159 S. M. Morton and L. Jensen, *J. Chem. Phys.*, 2010, **133**, 074103.
160 K. Kalyanasundaram and M. Grätzel, *Coord. Chem. Rev.*, 1998, **177**, 347–414.
161 M. Nazeeruddin, A. Kay, I. Rodicio, R. Humphry-Baker, E. Müller, P. Liska, N. Vlachopoulos and M. Grätzel, *J. Am. Chem. Soc.*, 1993, **115**, 6382–6390.
162 J.-F. Guillemoles, V. Barone, L. Joubert and C. Adamo, *J. Phys. Chem. A*, 2002, **106**, 11354–11360.
163 F. De Angelis, A. Tilocca and A. Selloni, *J. Am. Chem. Soc.*, 2004, **126**, 15024–15025.
164 M. Rekhis, F. Labat, O. Ouamerali, I. Ciofini and C. Adamo, *J. Phys. Chem. A*, 2007, **111**, 13106–13111.
165 S. Sauve, M. E. Cass, G. Goia, S. J. Doig, I. Lauermann, K. E. Pomykal and N. S. Lewis, *J. Phys. Chem. B*, 2000, **104**, 6821–6836.
166 L. C. T. Shoute and G. R. Loppnow, *J. Am. Chem. Soc.*, 2003, **125**, 15636–15646.
167 F. Labat, I. Ciofini, H. P. Hratchian, M. J. Frisch, K. Raghavachari and C. Adamo, *J. Phys. Chem. C*, 2011, **115**, 4297–4306.
168 H. P. Hratchian, P. V. Parandekar, K. Raghavachari, M. J. Frisch and T. Vreven, *J. Chem. Phys.*, 2008, **128**, 034107.
169 F. Labat, I. Ciofini, H. P. Hratchian, M. J. Frisch, K. Raghavachari and C. Adamo, *J. Am. Chem. Soc.*, 2009, **131**, 14290–14298.
170 F. Maseras and K. Morokuma, *J. Comput. Chem.*, 1995, **16**, 1170–1179.
171 I. Ciofini, P. P. Lainé, F. Bedioui and C. Adamo, *J. Am. Chem. Soc.*, 2004, **126**, 10763–10777.
172 S. Speiser, *Chem. Rev.*, 1996, **96**, 1953–1976.
173 G. D. Scholes, *Annu. Rev. Phys. Chem.*, 2003, **54**, 57–87.
174 J. L. Brédas, D. Beljonne, V. Coropceanu and J. Cornil, *Chem. Rev.*, 2004, **104**, 4971–5004.
175 T. Förster, *Ann. Phys.*, 1948, **6**, 55–75.
176 D. L. Dexter, *Phys. Rev.*, 1957, **108**, 630–633.
177 C. P. Hsu, M. Head-Gordon, T. Head-Gordon and G. R. Fleming, *J. Chem. Phys.*, 2001, **114**, 3065–3072.
178 M. F. Iozzi, B. Mennucci, J. Tomasi and R. Cammi, *J. Chem. Phys.*, 2004, **120**, 7029–7040.
179 M. E. Madjet, A. Abdurahman and T. Renger, *J. Phys. Chem. B*, 2006, **110**, 17268–17281.
180 B. P. Krueger, G. D. Scholes and G. R. Fleming, *J. Phys. Chem. B*, 1998, **102**, 5378–5386.
181 B. Mennucci and C. Curutchet, *Phys. Chem. Chem. Phys.*, 2011, **13**, 11538–11550.
182 C. Curutchet and B. Mennucci, *J. Am. Chem. Soc.*, 2005, **127**, 16733–16744.
183 C. Curutchet, A. Munoz-Losa, S. Monti, J. Kongsted, G. D. Scholes and B. Mennucci, *J. Chem. Theor. Comput.*, 2009, **5**, 1838–1848.
184 C. Curutchet, J. Kongsted, A. Munoz-Losa, H. Hossein-Nejad, G. D. Scholes and B. Mennucci, *J. Am. Chem. Soc.*, 2011, **133**, 3078–3084.
185 J. Neugebauer, *J. Chem. Phys.*, 2007, **126**, 134116.
186 J. Neugebauer, C. Curutchet, B. Munoz-Losa and B. Mennucci, *J. Chem. Theor. Comput.*, 2010, **6**, 1843–1851.
187 A. Munoz-Losa, C. Curutchet, I. F. Galvan and B. Mennucci, *J. Chem. Phys.*, 2008, **129**, 034104.

